CrossMark

Mapping QTLs and meta-QTLs for two inflorescence architecture traits in multiple maize populations under different watering environments

Xiaoqiang Zhao · Yunling Peng · Jinwen Zhang · Peng Fang · Boyang Wu

Abstract Drought significantly affects the architectural development of maize inflorescence, which leads to massive losses in grain yield. However, the genetic mechanism for traits involved in inflorescence architecture in different watering environments, remains poorly understood in maize. In this study, 19 QTLs for tassel primary branch number (TBN) and ear number per plant (EN) were detected in 2 $F_{2:3}$ populations under both well-watered and water-stressed environments by single environment mapping with composite interval mapping (CIM); 11/19 QTLs were detected under water-stressed environments. Moreover, 21 QTLs were identified in the 2 $F_{2:3}$ populations by joint analysis of all environments with a mixed linear model based on composite interval mapping (MCIM), 11 QTLs were involved in QTL × environment interactions, seven epistatic interactions were identified with additive by additive/dominance effects. Remarkably, 12 stable QTLs (sQTLs) were simultaneously detected by single environment mapping with CIM and joint analysis through MCIM, which were concentrated in ten bins across the chromosomes: 1.05_1.07, 1.08_1.10, 2.01_2.04, 3.01, 4.06, 4.09, 5.06_5.07, 6.05, 7.00, and 7.04 regions. Twenty meta-QTLs (mQTLs) were detected across 19 populations under 51 watering environments using a meta-analysis, and 34 candidate genes were predicted in corresponding mQTLs regions to be involved in the regulation of inflorescence development and drought resistance. Therefore, these results provide valuable information for finding quantitative trait genes and to reveal the genetic mechanisms responsible for TBN and EN under different watering environments. Furthermore, alleles for TBN and EN provide useful targets for marker-assisted selection to generate high-yielding maize varieties.

Xiaoqiang Zhao and Yunling Peng have contributed equally to this work.

X. Zhao · Y. Peng (✉) · J. Zhang · P. Fang · B. Wu
Gansu Key Lab of Crop Improvement and Germplasm Enhancement, Gansu Provincial Key Lab of Aridland Crop Science, College of Agronomy, Gansu Agricultural University, Lanzhou 730070, China
e-mail: pengyunlingpyl@163.com

Introduction

Maize (*Zea mays* L.) is a monoecious plant with an apical male inflorescence (tassel) and an axillary female inflorescence (ear). The tassel and ear are indispensable reproductive organs for corn production, and one of the most important traits in maize breeding (Lambert and Ohnson 1978; Upadyayula et al. 2006; Brown et al. 2011). The tassel typically provides more than enough pollen for fertilization, thus allowing plant breeders to select for smaller tassels without affecting fertility, thereby increasing light distribution in the field and

⌖ Springer

increasing the nutrients available for ear growth and yield (Upadyayula et al. 2006; Brown et al. 2011; Chen et al. 2014). Previous quantitative genetic studies suggest that indirect selection for yield through selection on ear traits, such as ear number per plant (EN), ear coarse, and ear length, can be more effective than directly selecting for yield (Ross et al. 2006; Huo et al. 2016).

Drought is one of the most important environmental stresses around the world, which severely affects maize growth during multiple developmental stages, especially during the transition from vegetative to reproductive growth (Xu et al. 2014). Previous studies show that inflorescence architecture is closely associated with drought tolerance in maize. Schoper et al. (1987) suggested that maize plants under heat and water stress had substantially lower pollen production and viability. Agrama and Moussa (1996) reported significant reductions in tassel primary branch number (TBN) and EN in 300 F_3 families under drought stress. Song and Dai (2005) and Li et al. (2005) revealed that tassel handle and tassel length were smaller, TBN and spikelet number were significantly decreased, and ears were smaller under drought stress. Gao et al. (2007) reported that male inflorescence traits, especially TBN and total tassel length in 183 F_3 families were significantly reduced under drought stress. Nikolic et al. (2011) described a decline in TBN of 116 F_3 families under drought conditions. Peng et al. (2014b) found that the anthesis-silking interval (ASI) was remarkably extended, and TBN was greatly decreased in drought sensitive maize after drought stress. Almeida et al. (2014) showed that EN was strikingly reduced and ASI was greatly extended in three populations under multiple drought conditions. In general, the TBN and EN are controlled by a large number of genetic loci/genes (Upadyayula et al. 2006; Gao et al. 2007; Almeida et al. 2014; Tanaka et al. 2013), which can be dissected as Mendelian factors using molecular markers. Several mapped populations were developed to identify quantitative traits loci (QTL) under multiple different watering environments, which can be used in marker-assisted selection (MAS) to improve drought tolerance in maize.

So far, many studies have been published to investigating TBN and EN (Agrama and Moussa 1996; Ribaut et al. 1997; Mickelson et al. 2002; Upadyayula et al. 2006; Gao et al. 2007; Nikolic et al. 2011; Zhang et al. 2013; Almeida et al. 2014; Zhang, et al. 2014; Wu et al. 2016); however, only limited QTLs for these traits have been identified under drought environments. Despite extensive research, the molecular mechanism of TBN and EN remains poorly understood, calling for in-depth investigations on the genetic mechanisms controlling TBN and EN under contrasting watering conditions. Past studies investigating maize lines under drought and normal conditions have clarified some of this mystery; Gao et al. (2007) identified six QTLs associated with TBN, Nikolic et al. (2011) mapped eight QTLs for TBN Agrama and Moussa (1996) detected three QTLs for EN, Ribaut et al. (1997) identified 12 QTLs for EN, and Almeida et al. (2014) performed the most thorough study to date and found 29 QTLs for EN (Supplementary Table S1). Creating a better understanding of the molecular mechanism of genetic variation of drought tolerance will be invaluable to breeding strategies to obtain higher yield. Furthermore, understanding this genotype by environment (G × E) interaction will provide a solid foundation for genetic improvement and optimization of genotypes across different environments, informing breeders of the QTL by environment (QTL × E) interaction (EI-Soda et al. 2014).

In the present study, we identify QTLs affecting TBN and EN in two $F_{2:3}$ populations under four well-watered and four water-stressed environments by single environment mapping with composite interval mapping (CIM). We then identify the joint QTL, epistatic interaction and QTL × E interaction among all environments in a joint analysis of both $F_{2:3}$ populations with a mixed linear model based on composite interval mapping (MCIM), We further identify meta-QTLs (mQTLs) for TBN and EN and predict possible candidate genes within these mQTLs intervals. This study can provide valuable information for the identification and characterization of genes involved in TBN and EN under different watering environments. These findings can be used to improve maize varieties through MAS for inflorescence architecture, and thereby alleviate global food crises resulting from drought.

Materials and methods

Plant materials

The two F_2 populations derived from Langhuang × TS141 and Chang7–2 × TS141 were used to construct the corresponding genetic linkage maps, which included 202 and 218 individuals. Then 202 and 218 $F_{2:3}$ family lines obtained by selfing individual F_2 plants, were used

to evaluate inflorescence traits (TBN and EN) and identify QTLs for corresponding traits across eight different watering environments. Three parents were chosen based on distant inflorescence architecture, drought resistance and maize germplasm groups. The strong drought tolerant inbred lines Langhuang and Chang7–2 originated from Tangsipingtou group as female parents. The drought sensitive inbred line TS141 derived from Reid yellow dent germplasm as the male parent for both (Peng et al. 2013; Peng et al. 2014b).

Field experiments and trait evaluation

The 202 $F_{2:3}$ family lines (LTpop) from Langhuang × TS141 and parents were evaluated under four watering environments at two locations in 2014 China, water-stressed environments at Wuwei (S-W: 37.97° N, 102.63° E; 1508 m altitude) and Zhangye (S-Z: 38.83° N, 106.93° E; 1536 m, altitude) and well-watered environments at Wuwei (W-W) and Zhangye (W-Z), respectively. The 218 $F_{2:3}$ family lines (CTpop) from Chang7–2 × TS141 and parents were measured under four watering environments at two locations in 2015 China: water-stressed environments at Gulang (S-G: 37.67° N, 102.85° E; 1785 m, altitude) and Jingtai (S-J: 37.18° N, 104.03° E; 1640 m, altitude) and well-watered environments at Gulang (W-G) and Jingtai (W-J). Each field followed a randomized complete block design with three replications. In each plot a single $F_{2:3}$ family line was planted in a row that was 6.0 m long and 0.6 m wide, with a total of 20 plants at a density of 55,580 plants ha^{-1}. Plastic film with 0.08 mm thick was laid over the fields where the width of plastic film covering on soil surface was 120 cm and plants were irrigated by drip irrigation. Water stressed plants were not irrigated from the beginning of the expected V18 stage to the end of expected R1 stage, although plants were irrigated at 20-day intervals in other developmental stages. Plants under well-watered environments were irrigated when rainfall was insufficient. The V18 stage is where the silks from the basal ear ovules elongate first, and brace roots (aerial nodal roots) grow from the nodes above the soil surface to sustain the plant and help in water and nutrients uptake during the reproductive stages. The R1 stage is the stage when silks are visible outside the husks; the silks serve the purpose of capturing pollen that falls from the tassel, and the captured pollen grain moves down the silk to the ovule, where pollination occurs (Ritchie et al. 1997). Lack of moisture during the time from V18 to R1 stages can cause poor pollination and kernel set.

For the two $F_{2:3}$ families and corresponding parents, ten consecutive plants from the middle of each plot were chosen to evaluate TBN (number of tassel primary branch) and EN (ear number per plant) at the end of R1 stage. Basic statistics and Pearson correlation analysis were performed on the phenotypic data from each watering condition. Analysis of variance (ANOVA) was employed to evaluate the total and residual variances among $F_{2:3}$ populations for each phenotypic trait. All analyses were performed using the IBM-SPSS Statistics 19.0. Broad-sense heritability (H^2) was calculated as follows (Knapp et al. 1985): $H^2 = \sigma_g^2 / \left(\sigma_g^2 + \sigma_{ge}^2/n + \sigma_e^2/nr \right)$ (1), where σ_g^2 represents the genetic variance, σ_{ge}^2 represents the genotype by environment interaction, σ_e^2 represents the error variance, r represents the replication number, and n represents the number of environments. The genetic correlation coefficients (r_g) were estimated as follows (Michael 1999): $r_g = COV_{gxy} / \sqrt{\sigma_{gx}^2 {}^* \sigma_{gy}^2}$ (2), where COV_{gxy} represents the covariance between x and y traits, σ_{gx}^2 or σ_{gy}^2 represents the genetic variance of x or y. The mid-parent heterosis (H_m) and over-parent heterosis (H_o) were estimated as follows: $H_m = (F_1 - MP)/MP^*100\%$ (3) and $H_o = (F_1 - P_L)/P_L{}^*100\%$ (4), where F_1 represents the value of the F_1 hybrid, MP represents the average value of both parents, and P_L represents the large value of parents (Gowda et al. 2010).

Genetic linkage maps construction and QTL analysis

Genomic DNA was extracted from young leaves of F_2 individuals and their corresponding parents using CTAB as described by Saghai-Maroof et al. (1984). A total of 213/217 polymorphic simple sequence repeat (SSR) markers out of 872 SSR markers covering the entire maize genome from the MaizeGDB (http://www.maizegdb.org) between Langhuang/Chang7–2 and TS141 were used to develop the genetic linkage maps with JoinMap version 4.0 (http://www.kyazma.nl/index.php/mc. JoinMap/sc.Evaluate/) (Van-Ooijen 2006). The Kosambi map function was used to calculate the genetic distances (centimorgan, cM).

QTL mapping for traits in each environment were performed by using Windows QTL Cartographer software version 2.5, with a composite interval mapping (CIM) approach (Wang et al. 2007). For CIM, model 6 of Zmapqtl module was used to identify QTLs. The window size was 10 cM and the cofactors were selected by forward and backward regressions with the in and out thresholds at a $P < 0.05$. A genome-wide critical threshold value for the experiment wise type I error rate of 0.05 was estimated with 1000 random permutations (Trachsel et al. 2009). The genetic action of each QTL was estimated by Stuber et al. (1987) as: $|d/a| = |dominance/additive|$; A, additive ($|d/a|$-0.00 ~ 0.20); PD, partial dominance ($|d/a| = 0.21 ~ 0.80$); D, dominance ($|d/a| = 0.81 ~ 1.20$); OD, over-dominance ($|d/a| > 1.20$). QTLs for traits were detected within the same marker interval or when confidence intervals (CIs) overlapped, the corresponding loci were assumed to be common QTLs with pleiotropic effects. QTLs repeatedly detected across the different environments or different mapping populations were considered as stable QTL (sQTL).

The joint QTL, epistatic interaction between QTLs for each trait at each environment and QTL by environment (QTL × E) interaction across all environments were identified by the QTL Network version 2.0, with a mixed linear model based on composite interval mapping (MCIM) approach (Yang et al. 2016). The testing window, walk speed and filtration window of genome scan were set at 10, 2, and 10 cM, respectively. One thousand permutation were performed to determine the threshold logarithm (base 10) of odds (LOD), for each trait for declaring a significant QTL at $P < 0.05$ probability level (Churchill and Doerge 1994). The name of the QTL was assigned according to the modifying nomenclature of McCouch et al. (1997). In addition, the letter "J" was labeled into the middle of this QTL name (namely, inserted between trait abbreviation and chromosome number), while one QTL was only detected in joint analysis with MCIM, but not in single environment through CIM program.

Consensus linkage map construction and meta-analysis

The corresponding mapping information from each QTL in our study under eight watering environments, and other 17 specific mapping information of QTLs for TBN and EN under 43 watering environments from public databases: MaizeGDB (http://www.maizegdb.org), National Center for Biotechnology Information (NCBI; http://www.ncbi.nlm.nih.gov/pubmed) and China National Knowledge Infrastructure (CNKI; http://www.cnki.net) (Supplementary Table S1), which included original chromosomal position, LOD score, confidence interval (CI), proportion of phenotypic variance (R^2), the value of TBN and EN, as well as the broad-sense heritability (H^2). A consensus linkage map was constructed by BioMercator version 4.2 (http://www.bioinformatics.org/mqtl/wiki) (Sosnowski and Joets 2012), and compared to the reference map IBM2 2008 Neighbors frame 6 (http://www.maizegdb.org/data_center/map). When the CI for QTL position was not available in a publication, a 90% CI was estimated as follows (Darvasi and Soller 1997): CI = 530/(N^*R^2) (5) or CI = 163/(N^*R^2) (6), where N represents the size of the mapping population and R^2 represents the phenotypic variance. Eq. (5) is appropriate for both backcross (BC) and F_2 populations, while eq. (6) is appropriate for the population of recombinant inbred lines (RILs).

After the QTLs in the original populations were identified with a homothetic function, they were projected on a consensus map, and multiple algorithms for meta-analysis were used to estimate the number, position, and akaike information criterion (AIC) 95% CI of the mQTLs with BioMercator version 4.2 (Sosnowski and Joets 2012). Then mQTLs were projected on the physical reference map B73 RefGen_v2 (http://www.maizegdb/gbrowse/maize_V2) to identify candidate genes.

Results

Inflorescence architecture traits analysis

In this study, we explored the QTLs associated with changes in tassel primary branch number (TBN) and ear number per plant (EN) in three parents and two $F_{2:3}$ populations (LTpop and CTpop) under eight watering environments (W-W, W-Z, W-G, W-J, S-W, S-Z, S-G, and S-J). For the three corresponding parents, under well-watered environments, the drought tolerant female parents Langhuang/Chang7–2 had a larger TBN and EN than the TS141 intolerant male parent, 9.56/10.58 vs. 19.62 and 1.79/1.31 vs. 2.03, respectively. However,

under water-stressed environments, TBN and EN in Langhuang, Chang7–2 and TS141 were on average reduced by 19.87, 17.86, and 30.89% and by 11.73, 11.45, and 36.71%, respectively (Table 1; Supplementary Fig. S1). As expected, under drought stressed conditions the drought sensitive parent TS141 had greater reductions in TBN and EN than drought tolerant parents (Langhuang and Chang7–2). Furthermore, compared with the three parents, uniform changes for TBN and EN occurred in the two $F_{2:3}$ populations under water-stressed environments, TBN and EN were on average reduced by 18.33 and 12.28%, and by 14.72 and 10.54% in LTpop and CTpop, respectively (Table 1; Supplementary Fig. S1). In addition, TBN and EN in LTpop and CTpop were normally distributed under eight watering environemts (Table 1; Supplementary Fig. S2). Approximately 32.57 ~ 56.13% for variation in TBN and EN were attributed to genetic variations, significantly more than the 7.23 ~ 23.61% of environmental variations in LTpop and CTpop (Supplementary Fig. S2). The broad-sense heritability (H^2) for TBN and EN in LTpop and CTpop were predominantly high at 75.31 ~ 84.28%, respectively (Table 1).

Correlation among tested traits

In this study, we revealed the phenotypic (r_p) and genetic (r_g) correlation among tested traits in the two $F_{2:3}$ populations (LTpop and CTpop), respectively. These tested traits included two inflorescence architecture traits (TBN and EN) and another four secondary traits of drought tolerance, namely ASI, ear weight (EW), 100-kernel weight (KW), and ear length (EL). For the two $F_{2:3}$ populations, TBN had negative correlation with ASI (r_p= −0.343 and r_g= −0.374, average), EN (r_p= −0.144 and r_g= −0.175, average), and had positive correlation with EW (r_p= 0.331 and r_g= 0.359, average), KW (r_p= 0.271 and r_g= 0.321, average) and EL (r_p= 0.239 and r_g= 0.259, average), respectively. ASI had negative correlation with EW (r_p= −0.446 and r_g= −0.504, average), KW (r_p= −0.134 and r_g= −0.186, average) and EL (r_p= −0.355 and r_g= −0.432, average), and had positive correlation with EN (r_p= 0.234 and r_g= 0.286, average), respectively. EN had positive correlation with EW (r_p= 0.305 and r_g= 0.346, average), KW (r_p= 0.312 and r_g= 0.359, average) and EL (r_p= 0.213 and r_g= 0.267, average), respectively. EW had positive correlation with KW (r_p= 0.610 and r_g= 0.696, average) and EL (r_p= 0.547 and r_g= 0.608, average), respectively.

KW had negative correlation with EL (r_p= −0.368 and r_g= −0.447, average) (Supplementary Table S2). This may indicate that inflorescence architecture plasticity in maize is the result of the synergistic effect of tassel and ear, and inflorescence architecture traits are closely associated with secondary traits of drought tolerance, thus, we can use inflorescence architecture to reveal the drought tolerance mechanism in maize.

SSR data analysis and genetic linkage maps construction

Genetic linkage maps were developed for two corresponding F_2 populations for QTL mapping. In this study, 213 genome-wide polymorphic SSR markers were used for genotyping the 202 F_2 individuals derived from Langhuang × TS141, 199 of which followed the expected 1:2:1 ratio. The genetic linkage map spanned a total length of 1542.5 cM with an average interval of 7.8 cM between markers (Fig. 1). Similarly, 217 genome-wide polymorphic SSR markers were used for genotyping of the 218 F_2 plants derived from Chang7–2 × TS141, of which 205 SSRs fitted the expected 1:2:1 ratio. The genetic linkage map was 1648.8 cM with an average distance of 8.0 cM between markers (Fig. 2). Most of markers on the two maps were consistent with the bin locations in the IBM2 2008 Neighbors map frame 6 (http://www.maizegdb.org/data_center/map).

QTL mapping for TBN and EN in a single environment

Using single environment mapping with CIM, we detected 19 significant ($P < 0.05$) QTLs (12 TBN-QTLs and 7 EN-QTLs) across two $F_{2:3}$ populations (LTpop and CTpop) under eight watering environments (W-W, W-Z, W-G, W-J, S-W, S-Z, S-G, and S-J). Eleven of 19 QTLs (seven TBN-QTLs and four EN-QTLs) were detected under water-stressed environments (Supplementary Table S3; Figs. 1 and 2). For LTpop, six TBN-QTLs were mapped on chromosomes 3, 4, 6, 7, and 9, which explained 4.29 ~ 23.24% of phenotypic variance (R^2) in a single environment. All QTLs for TBN had partial dominance (54.5%) and overdominance (45.5%). Approximately 63.6% of alleles decreasing TBN were contributed by female parent Langhuang. Five EN-QTLs were identified on chromosomes 1, 4, 6, and 10, which explained 4.12 ~ 26.95% of R^2 in a single environment. Most of EN-QTLs were additive (40.0%) and dominance (40.0%).

Table 1 Analysis of TBN and EN in LTpop and CTpop under different watering environments, respectively

Traits[#]	Env[&]	Parents		F$_{2:3}$ population					H^2 (%)[$]	90% CI[¥]
				Mean	Range	CV (%)[†]	Skewness	Kurtosis		
		Langhuang	TS141	LTpop (No. of LTpop = 202)						
TBN	W-W	9.17 ± 0.88	16.46 ± 1.05	14.94 ± 2.96	8.00–22.67	19.84	0.170	−0.350	78.69	76.21–80.08
(No.)	S-W	7.30 ± 1.01	11.31 ± 1.00	12.66 ± 2.71	5.00–20.40	21.38	0.092	0.418		
	W-Z	9.94 ± 1.10	18.97 ± 1.47	16.71 ± 3.18	7.80–25.33	19.01	0.273	−0.128		
	S-Z	8.01 ± 0.93	12.06 ± 1.09	13.19 ± 3.15	4.00–23.00	23.92	0.331	0.340		
EN	W-W	1.75 ± 0.50	1.80 ± 0.45	2.83 ± 0.68	1.00–5.00	23.96	0.356	0.768	75.31	73.17–76.97
(No.)	S-W	1.50 ± 0.57	1.40 ± 0.54	2.25 ± 0.53	1.00–3.50	23.65	−0.188	−0.345		
	W-Z	1.83 ± 0.41	2.16 ± 0.41	3.08 ± 0.76	1.00–5.67	24.73	0.446	0.809		
	S-Z	1.66 ± 0.52	1.50 ± 0.55	2.79 ± 0.73	1.00–4.67	26.27	−0.459	0.646		
		Chang7–2	TS141	CTpop (No. of CTpop = 218)						
TBN	W-G	11.15 ± 2.41	22.39 ± 4.05	21.34 ± 4.86	8.00–33.00	22.79	−0.145	−0.119	84.26	83.04–85.98
(No.)	S-G	9.14 ± 2.03	16.95 ± 3.20	18.35 ± 5.44	7.00–30.00	29.67	−0.185	−0.692		
	W-J	10.00 ± 2.92	20.62 ± 3.43	19.46 ± 5.64	8.00–34.00	28.97	−0.059	−0.353		
	S-J	8.23 ± 2.27	13.93 ± 2.61	17.44 ± 5.96	5.00–31.00	34.17	−0.223	−0.607		
EN	W-G	1.33 ± 0.52	2.00 ± 0.89	2.81 ± 0.73	1.00–5.00	26.06	0.212	0.795	84.28	81.93–86.35
(No.)	S-G	1.17 ± 0.41	1.33 ± 0.52	2.67 ± 0.78	1.00–4.67	29.37	−0.452	0.152		
	W-J	1.28 ± 0.49	2.14 ± 0.90	2.79 ± 0.88	1.00–5.20	31.49	−0.283	0.074		
	S-J	1.14 ± 0.38	1.29 ± 0.49	2.34 ± 0.61	1.00–4.00	26.24	0.299	0.386		

[#] Traits: *TBN (No.)* Tassel primary branch number; *EN (No.)* Ear number per plant

[&] Env (environment): *W-W* Well-watered environment at Wuwei; *S-W* Water-stressed environment at Wuwei; *W-Z* Well-watered environment at Zhangye; *S-Z* Water-stressed environment at Zhangye; *W-G* Well-watered environment at Gulang; *S-G* Water-stressed environment at Gulang; *W-J* Well-watered environment at Jingtai; *S-J* Water-stressed environment at Jingtai

[†] *CV (%)* Coefficient of variation

[$] *$H^2$ (%)* Broad-sense heritability

[¥] *90% CI* Confidence intervals of broad-sense heritability between 5 and 95% significant levels

The same as below

Approximately 60.0% of alleles decreasing EN were contributed by female parent Langhuang. For CTpop, six TBN-QTLs were located on chromosomes 2, 4, 5, 6, 7, and 9, which explained 4.22 ~ 17.85% of R^2 in a single environment. These TBN-QTLs were additive (54.5%) and over-dominance (45.5%). Approximately 72.7% of alleles decreasing TBN were contributed by female parent Chang7–2. Two EN-QTLs were detected on chromosomes 3 and 6, which explained 6.18 ~ 17.42% of R^2 in a single environment. Most of EN-QTLs had additive effect (60.0%). Approximately 80.0% of alleles decreasing EN were contributed by female parent Chang7–2.

QTL mapping for TBN and EN in joint analysis among all environments

Using joint analysis of all environments with MCIM, we detected 21 significant ($P < 0.05$) QTLs (11 TBN-QTLs and 10 EN-QTLs) in two F$_{2:3}$ populations (LTpop and CTpop) (Table 2); 13/21 QTLs were also identified in single environment mapping. The additive effect of each significant QTL ranged from −2.10 to 1.94, which explained 3.14 ~ 13.35% of phenotypic variance [h^2(A)]. In addition, 11 significant ($P < 0.05$) QTLs (four TBN-QTLs and seven EN-QTLs) were involved in QTL × E interactions, which accounted for 2.94 ~ 7.96% of the phenotypic variance [h^2(AE)]. This may indicate that the QTLs main effects may have stronger effects on
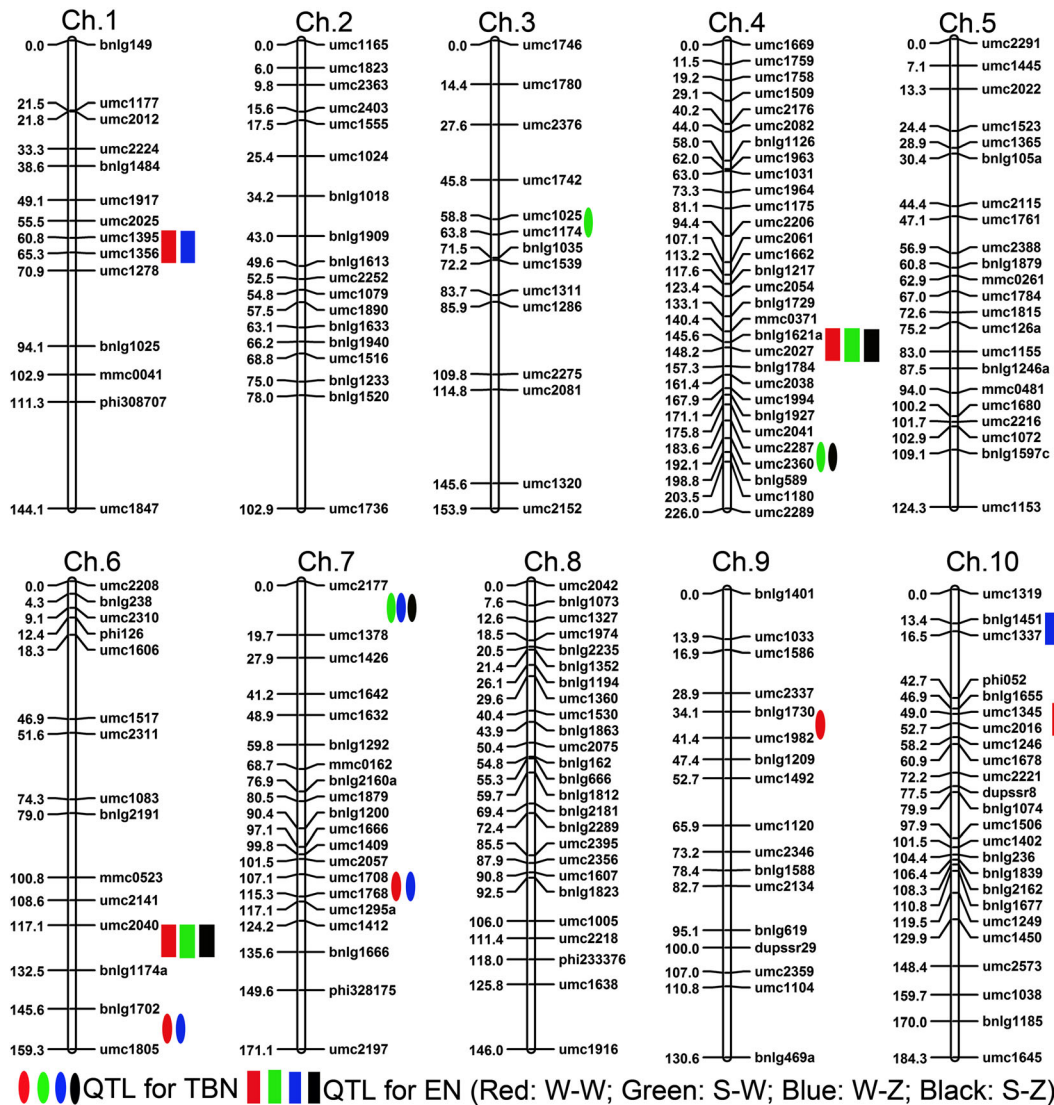
Fig. 1 Molecular linkage map construction and QTLs detected for TBN and EN in LTpop by single environment mapping with CIM

TBN and EN. Remarkably, chromosomal bin 1.08_1.10 (mmc0041-phi308707) exhibited stable QTL × E interaction for EN in the two $F_{2:3}$ populations, which implies that this region may be mediated by environmental factors. In addition, 12 sQTLs (seven TBN-sQTLs and five EN-sQTLs) were identified in the two $F_{2:3}$ populations by both single environment mapping with CIM and joint analysis through MCIM. These were dispersed on chromosomes 1, 2, 3, 4, 5, 6, and 7. Each sQTL explained 3.14 ~ 19.96 (sQTL11) to 7.41 ~ 13.35% (sQTL1) of phenotypic variance (R^2). Six of 12 sQTLs (sQTL2, 3, 4, 6, 11, and 12) were detected under water-

stressed environments. Notably, one common sQTL was identified in bin 1.08_1.10 (mmc0041 and phi308707) that demonstrated a pleiotropic effect on TBN and EN, which may indicate that bin 1.08_1.10 may be an important region in regulating inflorescence architecture (Supplementary Table S4).

Epistatic interaction

Out of all QTLs identified, three pairs of significant ($P < 0.05$) epistatic interactions for TBN were identified with additive by additive (AA) effects among all
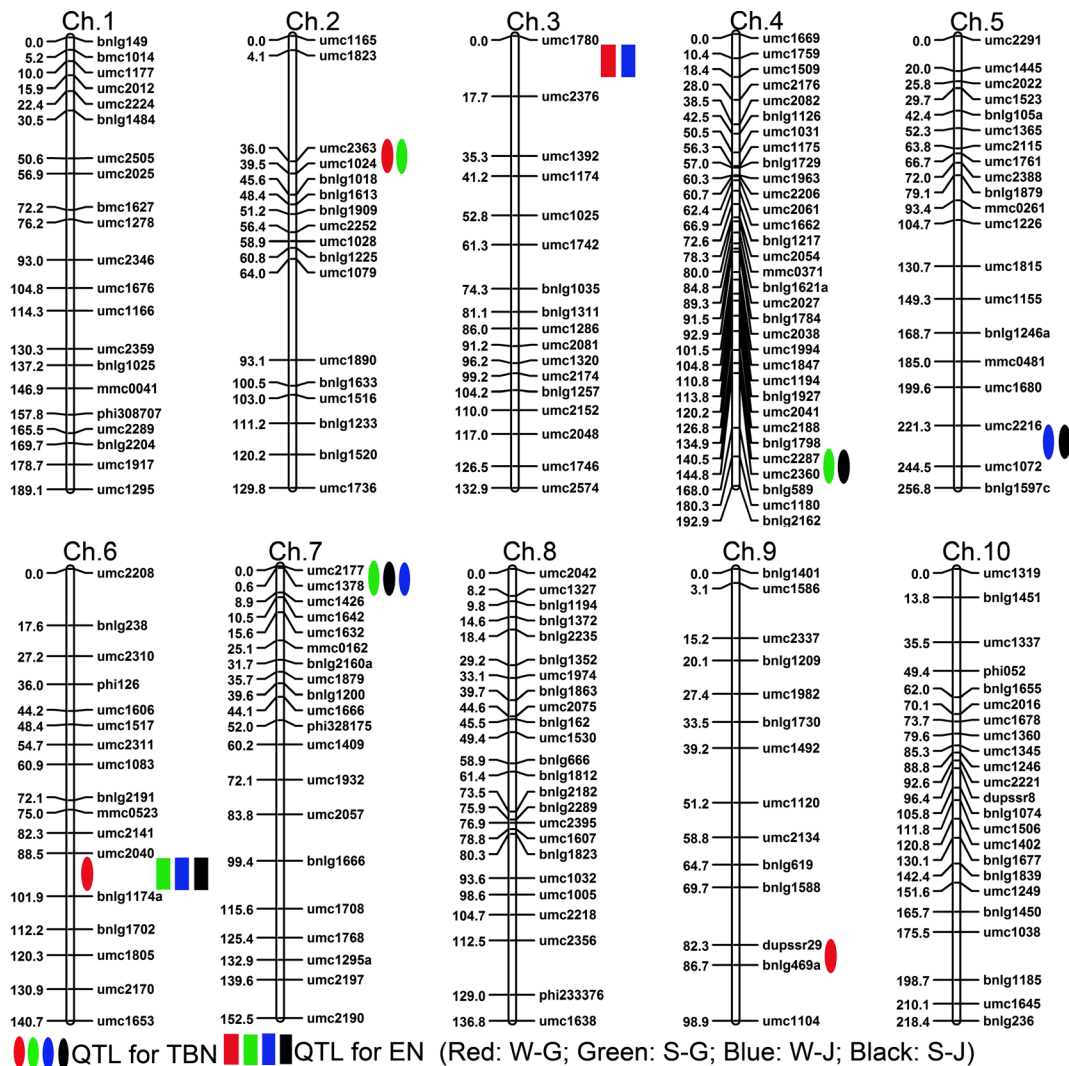
Fig. 2 Molecular linkage map construction and QTLs detected for TBN and EN in CTpop by single environment mapping with CIM

environments in the two $F_{2:3}$ populations (LTpop and CTpop). These were simultaneously located between bin 1.08 1.10 (mmc0041-phi308707) and bin 4.09 (umc2287-umc2360), and explained 6.15, 6.03, and 5.07% of phenotypic variance [h^2(AA)], respectively (Supplementary Table S5). Moreover, three pairs of significant ($P < 0.05$) epistatic interactions for EN were identified with AA effects and one pair of significant ($P < 0.05$) epistatic interaction for EN was identified with additive by dominance (AD) effect among all environments in the two $F_{2:3}$ populations, which explained 3.71 ~ 5.79% of phenotypic variance [h^2(AA)] and 3.94% of phenotypic variance [h^2(AD)], respectively (Supplementary Table S5).

Information analysis of TBN and EN in multiple original progeny populations

We integrated our analysis of TBN and EN with 19 original progeny populations (2 F_2, 10 $F_{2:3}$, 4 F_3, 2 RILs, and 1 BC_1S_1) from previous studies in hopes to reveal genetic mechanism of TBN and EN across 36 normal and 15 drought environments (Supplementary Table S1; Supplementary Fig. S3). Under normal environments, the average of TBN was 13.46 (CV = 29.79%), 15.71 (CV = 33.86%), and 16.52 (CV = 24.56%) in female parents, male parents, and progeny populations, respectively. The average of EN was 1.48 (CV = 26.16%), 1.72 (CV = 32.82%), and 1.76 (CV = 54.46%),

Table 2 QTLs for TBN and EN were detected in LTpop and CTpop by joint analysis among all environments with MCIM

Trait	QTL	Chr.	QTL position			A[b]	AE1[c]	AE2[c]	AE3[c]	AE4[c]	h²(A)(%)[d]	h²(AE)(%)[e]
			cM	Mb[a]	Marker interval							
LTpop (No. of LTpop = 202)												
TBN	qTBN-J1–1[f]	1	110.8	17.51	mmc0041-phi308707	−2.10					13.35	
	qTBN-J2–1	2	55.1	39.86	umc1079-umc1890	1.03	0.75				6.12	5.88
	qTBN-Ch.4–1	4	190.9	3.41	umc2287-umc2360	1.94					10.56	
	qTBN-Ch.6–1	6	147.3	1.83	bnlg1702-umc1805	1.16					6.98	
	qTBN-Ch.7–1	7	11.2	1.58	umc2177-umc1378	−2.07					13.11	
	qTBN-Ch.7–2	7	109.7	1.58	umc1708-umc1768	−0.68	−0.47		−0.39		5.73	4.05
EN	qEN-Ch.1–1	1	62.4	41.16	umc1395-umc1356	−2.10				−1.32	13.24	7.96
	qEN-J1–2	1	109.0	17.51	mmc0041-phi308707	−1.87	−1.00	−1.17		−1.04	10.12	6.28
	qEN-J2–1	2	2.1	4.95	umc1165-umc1823	1.00					6.07	
	qEN-Ch.4–1	4	148.0	0.85	bnlg1621a-umc2027	−0.33					3.14	
	qEN-Ch.6–1	6	131.4	11.12	umc2040-bnlg1174a	0.51	0.37	0.40		0.36	4.63	3.31
CTpop (No. of CTpop = 218)												
TBN	qTBN-J1–1	1	152.6	17.51	mmc0041-phi308707	−1.54					7.41	
	qTBN-Ch.2–1	2	37.9	24.52	umc2363-umc1024	−0.93	−0.66	−0.40			5.14	3.57
	qTBN-Ch.4–1	4	141.1	3.62	umc2287-umc2360	−1.37					6.40	
	qTBN-Ch.5–1	5	230.7	2.96	umc2216-umc1072	0.40		0.32	0.26	0.30	3.58	2.94
	qTBN-Ch.7–1	7	0.2	1.58	umc2177-umc1378	−1.75					9.53	
EN	qEN-J1–1	1	153.0	17.51	mmc0041-phi308707	−1.24		−0.98		−0.75	6.16	4.92
	qEN-Ch.3–1	3	17.2	1.89	umc1780-umc2376	−1.31					6.29	
	qEN-Ch.6–1	6	93.7	11.12	umc2040-bnlg1174a	−1.63		−1.31	−1.07	−1.08	8.87	5.81
	qEN-J8–1	8	77.4	0.75	umc2395-umc1607	1.55	−0.93				7.47	5.11
	qEN-J10–1	10	70.9	65.32	umc2016-umc1678	−1.00	−0.67	−0.39			5.32	3.56

[a] *Mb* The estimated physical distance of marker interval

[b] *A* The additive effect of QTL

[c] *AE1–4* The additive by designated environment (1: W-W, 2: S-W, 3: W-Z, 4: S-Z in the LTpop; 1: W-G, 2: S-G, 3: W-J, 4: S-J in the CTpop) interaction effect

[d] *h² (A)* Phenotypic variance explained by the QTL across all environments

[e] *h² (AE)* Phenotypic variance explained by the additive by designated environment interaction effect

[f]: The letter J was inserted in the name of one QTL, indicating that the QTL was detected only by joint analysis among all environments, but not a single-environmental QTL

respectively. Under drought conditions the average value for TBN and EN were significantly reduced in female parents, male parents and all progeny populations. The average of TBN was 8.10 (CV = 8.37%), 12.71 (CV = 22.76%), and 14.79 (CV = 19.42%), respectively. The average of EN was 1.18 (CV = 29.96%), 1.10 (CV = 41.13%), and 1.60 (CV = 54.93%), respectively (Supplementary Fig. S3). In addition, the average of broad-sense heritability (H^2) for TBN and EN were 81.42 (CV = 9.22%) and 77.20 (CV = 6.72%), respectively (Supplementary Fig. S3). Furthermore, the average of mid-parent heterosis (H_m) for TBN and EN were 36.80 (CV = 44.75%) and 63.97% (CV = 26.41%), respectively. The average of over-parent heterosis (H_o) for TBN and EN were 19.42 (CV = 74.59%) and 52.85% (CV = 34.39%), respectively (Supplementary Fig. S3).

Consensus map development and meta-QTLs (mQTLs) detection

A consensus map was constructed across the 19 populations to detect mQTLs for TBN and EN,

and candidate genes were predicted in corresponding mQTLs intervals to lay the foundation for fine mapping and MAS (Supplementary Table S1). The size of the 19 mapping populations varied from 116 to 330 with an average of 231.3. The map length of the mapping populations ranged from 868.7 to 3558.3 cM with an average of 1940.4 cM. The number of markers in per population varied from 70 to 376 with an average of 179.5 (Supplementary Table S1). The 213 original QTLs (152 TBN-QTLs and 61 EN-QTLs) were detected in these 19 original populations under 36 normal and 15 drought environments using four mapping approaches (Supplementary Table S1). These TBN/EN-QTLs were located on all ten chromosomes (Supplementary Fig. S3). Most of gene action for TBN-QTLs were additive effect (32.26%) and partial dominance effect (40.32%). Most of gene action for EN-QTLs were partial dominance (20.69%) and over-dominance effect (44.83%) (Supplementary Fig. S3). The LOD score per TBN/EN-QTL in mapping populations ranged from 2.30 to 25.13 with an average of 6.02. The phenotypic variance explained by each TBN/EN-QTL (R^2) in mapping populations varied from 1.18 to 32.28% with an average of 8.89% (Supplementary Fig. S3).

The consensus linkage map was constructed using BioMercator version 4.2 with the IBM2 2008 Neighbors map frame 6, which was 7246.90 cM length with an average interval of 11.10 cM between markers (Supplementary Table S6). The number of markers per chromosome in the consensus map ranged from 51 to 99, with an average of 65.3 markers. Then 103 TBN-QTLs (67.8%) and 37 EN-QTLs (60.8%) were successfully projected on this consensus map (Supplementary Table S6). In addition, using a meta-analysis we detected 20 mQTLs on chromosomes 1 (4 mQTLs), 2 (3 mQTLs), 3 (3 mQTLs), 4 (3mQTLs), 5 (1 mQTL), 6 (1 mQTL), 7 (2 mQTLs), 8 (1 mQTL), 9 (1 mQTL), and 10 (1 mQTL). Mean phenotypic variance explained by each mQTL varied from 4.4 to 20.9% with an overall average of 8.9%. The mean physical distance of each mQTL interval ranged from 0.7 to 77.8 Mb with an average of 9.3 Mb (Table 3; Supplementary Fig. S4). Furthermore, the corresponding 20 mQTLs were projected on the physical map B73 RefGen_v2 (http://www.maizegdb/gbrowse/maize_V2), resulting in the identification of 34 candidate genes (Table 3).

Discussion

The genetic characteristics of inflorescence architecture and breeding selection

Inflorescence architecture, such as TBN and EN are typical quantitative traits and play a crucial role in determining grain yield (Veldboom and Lee 1994; Duvick et al. 2004; Gao et al. 2007; Fan et al. 2012; Bartlett and Thompson 2014), thus genetic insight into TBN and EN is important for breeding high-yielding maize varieties. Duvick and Cassman (1999) reported that the tassel of pioneer hybrids had decreased by 36% over 30 years, which seems to be an ongoing trend (Sun et al. 2012). In general, high-yielding varieties have 1 ~ 2 EN, as too much or too little EN could lead to reduction in yield (Li et al. 2011; Hu et al. 2012). Moreover, there was a large broad-sense heritability (H^2) and positive mid/over-parent heterosis (H_m/H_o) of TBN and EN (Supplementary Fig. S3). Most of the gene action of TBN-QTLs were additive and partial dominance effects, and a large proportion of the gene action EN-QTLs were partial dominance and over-dominance effects (Supplementary Fig. S3) (Agrama and Moussa. 1996; Ribaut et al. 1997; Mickelson et al. 2002; Tang et al. 2005; Upadyayula et al. 2006; Gao et al. 2007; Nikolic et al. 2011; Wang et al. 2011; Zhang et al. 2013; Almeida et al. 2014; Zhang et al. 2014; Dong et al. 2015). Hence, in order to obtain genotypes with small tassels and a moderate number of ears in maize breeding, strong selection should be employed in early generations from base materials.

The QTL relationships between inflorescence architecture and drought tolerance

Drought can significantly affect the growth and development of tassels and ears in maize (Ribaut et al. 1997; Nikolic et al. 2011; Almeida et al. 2014). Many traits are negatively impacted by drought, including TBN, spikelet number, total tassel length, tassel handle length, pollen amount, pollen viability, tasseling time, silking time, EN, ear length, and ear thickness (Agrama and Moussa 1996; Ribaut et al. 1997; Song and Dai 2005; Li et al. 2005; Gao et al. 2007; Hu et al. 2008; Nikolic et al. 2011; Hu et al. 2012; Almeida et al. 2014; Peng et al. 2014b). This study has revealed that TBN and EN were

Table 3 The meta-analysis of QTLs for TBN and EN in maize and candidate genes prediction in corresponding mQTLs intervals under different environments

Traits	No. of QTLs		mQTLs	Bin	Position (cM)	Confidence interval (cM)	Adjacent markers	Mean LOD score of the original QTLs	Mean R^2 of the original QTLs (%)	Physical distance (Mb)	Physical interval (Mb)	Contig	Candidate genes
	NE	DE											
EN	6		mQTL1-1	1.05–1.05	460.6	453.8–461.3	umc1676-umc1395	13.7	20.9	148.6–164.6	15.9	ctg31-ctg34	MEM1
TBN	7		mQTL1-2	1.10–1.10	915.3	904.5–921.9	umc1885-phi308707	4.8	4.4	258.9–274.7	15.8	ctg57-ctg58	EXG1, ZMM4
EN	2	2	mQTL1-3	1.10–1.10	961.4	950.4–963.0	phi308707-umc161a	4.2	9.7	274.7–283.2	8.5	ctg58-ctg61	lem1, MYB78, opaque2
TBN	5		mQTL1-4	1.12–1.12	1128.7	1124.6–1131.6	umc1605-umc1797	6.4	4.8	298.7–300.8	2.1	ctg66-ctg67	vp8
TBN	4		mQTL2-1	2.02–2.02	94.5	83.7–109.1	umc2403-umc1934	7.5	5.3	5.4–10.2	4.8	ctg69-ctg70	MROS1, APO1
TBN, EN	5	4	mQTL2-2	2.05–2.05	350.3	343.1–357.4	umc131-umc1028	3.4	7.7	71.1–148.9	77.8	ctg82-ctg90	DBEs, MYB78, LOXs
TBN	2		mQTL2-3	2.09–2.10	714.9	694.7–717.3	umc2184-umc2214	3.4	8.6	234.3–235.1	0.8	ctg109-ctg110	Hd1
EN	5		mQTL3-1	3.01–3.01	36.3	30.2–41.7	umc2071-umc2376	5.5	7.8	2.8–3.5	0.7	ctg111-ctg111	opaque2
TBN	6		mQTL3-2	3.04–3.04	186.2	183.8–190.0	umc1392-umc1025	5.3	8	21.9–27.7	5.9	ctg115-ctg115	OCL1
EN	1	7	mQTL3-3	3.09–3.09	729.7	724.1–735.7	bnlg1257-umc2152	3.1	11.6	217.9–219.6	1.7	ctg149-ctg149	fdl1
TBN	3	3	mQTL4-1	4.03–4.04	174.8	163.1–190.9	umc2176-umc1117	7.8	5.3	17.4–25.2	7.8	ctg160-ctg160	RAT1, RAT2, FLO-LFY, FRRP1
TBN, EN	6		mQTL4-2	4.06–4.06	351.1	343.6–359.7	bnlg1621a-bnlg1784	7.7	11.7	153.7–162.9	9.2	ctg181-ctg182	ZAG3, LOXs
TBN	2	1	mQTL4-3	4.09–4.09	600.5	595.3–612.7	umc2287-umc1101	9	16.7	231.9–236.2	4.3	ctg198-ctg201	SPL3, LOXs, CaMBP
TBN	1	1	mQTL5-1	5.06–5.07	573.5	567.1–592.3	umc2216-umc1072	3.8	5.4	202.5–205.4	2.9	ctg250-ctg253	SNAC3
EN	2	4	mQTL6-1	6.05–6.05	290	287.2–291.7	umc2040-bnlg1174a	6.8	9.8	133.2–144.3	11.1	ctg285-ctg269	lg3, EF-1 alpha, GST
TBN	2	4	mQTL7-1	7.00–7.00	21.9	11.6–27.3	umc2177-umc1378	8.8	13.4	1.3–2.8	1.6	ctg293-ctg293	MADS3, OsCIN1, HSP3
TBN	2	1	mQTL7-2	7.04–7.04	460.1	427.5–491.8	umc1710-umc1295a	3.8	5.2	156.6–165.3	8.7	ctg323-ctg325	lg3, E13

Table 3 (continued)

Traits	No. of QTLs^		mQTLs	Bin	Position (cM)	Confidence interval (cM)	Adjacent markers	Mean LOD score of the original QTLs	Mean R² of the original QTLs (%)	Physical distance (Mb)	Physical interval (Mb)	Contig	Candidate genes
	NE	DE											
EN	2		mQTL8-1	8.06–8.06	430.4	424.1–435.8	bnlg240–mmc0181	3.9	9.5	162.6–164.9	2.3	cg361–ctg362	ald1, ig1, OsSIK2,
TBN	3		mQTL9-1	9.01–9.02	95.1	90.2–101.5	umc1588–umc1170	5.2	5	11.5–13.2	1.6	ctg373–ctg373	ZAG4
EN	1		mQTL10-1	10.01–10.02	78.6	70.4–89.9	bnlg1451–phi063	4.2	8.1	4.6–6.8	2.2	ctg392–ctg393	cr4
Total/Mean	65/–	29/–	20/–		–/432.7			–/5.9	–/8.9	–/9.3			34/–

^No. of QTLs (NE/DE): No. of identified QTLs in corresponding mapping populations across normal/drought environment

reduced under drought stress in both $F_{2:3}$ populations and parents. Moreover, with drought stress TBN and EN were reduced much more in the drought sensitive parent (TS141) than in the drought tolerant parents (Langhuang and Chang7–2).

So far, few studies of TBN-QTLs (two) and EN-QTLs (three) under drought environments have been reported (Agrama and Moussa 1996; Ribaut et al. 1997; Gao et al. 2007; Nikolic et al. 2011; Almeida et al. 2014). However, we find that the QTLs for TBN and EN show relatively small effects and sometimes cannot be mapped in other genetic backgrounds. Thus, in a specific genetic background show relatively small effects or even cannot be mapped under other genetic backgrounds, and the genetic mechanism of TBN and EN remains poorly understood in maize. Thus, in this study we mapped 19 QTLs for TBN and EN based on the two $F_{2:3}$ populations under eight watering environments using single environment mapping with CIM. Eleven of 19 QTLs were identified under water-stressed environments, and 21 significant QTLs were identified in the two $F_{2:3}$ populations using a joint analysis across all environments with MCIM. Moreover, 11 QTLs were involved in significant QTL × E interactions. One stable QTL × E interaction for EN in the two $F_{2:3}$ populations was located in bin 1.08_1.10 (mmc0041-phi308707), verifying previous results (Lu et al. 2007) showing a QTL × E interaction for ear length was located in bin 1.09_1.10 (bnlg1331-phi308707), indicating that this region mediates an interaction between the ear and the environment. In addition, 12 sQTLs were identified in the two $F_{2:3}$ populations, six of which were detected in water-stressed environments. These sQTLs can provide reliable information for breeding and future studies on the genetics of TBN and EN.

Epistasis between QTLs

Epistasis, or interaction effects between a pair of loci may play fundamental roles in broadening our understanding of the genetic structure behind complex quantitative traits (Phillips 2008). In this study, all phenotypic variance was explained by all significant QTLs, but were always less than the corresponding broad-sense heritability, regardless of the trait. This reveals that the missing proportion of phenotypic variance may be partly

explained by epistasis (Ma et al. 2007). Lan (2010) reported that 25 epistatic interactions for anthesis time, silking time and ASI were identified with additive by additive (AA), additive by dominance (AD), dominance by additive (DA), and dominance by dominance (DD) effects. In this study, three significant epistatic interactions for TBN were identified showing AA effects, which were simultaneously located in the region between bin 1.08_1.10 (mmc0041-phi308707) and bin 4.09 (umc2287-umc2360). This implies that the region between bin 1.08_1.10 and bin 4.09 may be an epistatic regulator that acts on male inflorescence development in maize. Considered as epistatic regulator which acted on the male inflorescence development in maize. Lu et al. (2007) suggested that four epistatic interactions for ear length were identified with AA, AD, DA, and DD effects. Yang et al. (2015) found that two epistatic interactions for ear row number were identified with AA effects. Yang et al. (2016) showed that one epistatic interaction for 100-kernel weight demonstrated an AA effect. We identified one significant epistatic interactions for EN with AD effect and three significant epistatic interactions for EN with AA effects. Thus, indicating that AA and AD may be the main epistatic interaction effects for EN.

Detection of mQTLs for inflorescence architecture and candidate genes prediction

The in-depth integration and meta-analysis of QTLs is informative for understanding the molecular mechanism and predicting candidate genes underpinning TBN and EN. Here, we integrated 19 mapping data sources under 51 watering conditions to develop a consensus map spanning 7246.90 cM. We detected 20 mQTLs for TBN and EN, which contained 34 candidate genes. The 20 mQTLs and 34 candidate genes reported here deserve further investigation using integrated omics and systems biology.

On chromosome 1, the MEM1 protein was mapped within the mQTL1–1 interval (15.9 Mb) between umc1676 and umc1395, affecting EN under six normal environments. Interestingly, the sQTL8 for EN was also located in the same interval. The MEM1 protein (maize endosperm motif binding protein) is specifically expressed in maize seeds (Heyl et al. 2001). The ZMM4 gene and homologous EXG1gene were found in the mQTL1–2

region (15.8 Mb) between umc1885 and phi308707, which may explain TBN and EN variation in seven normal environments. The sQTL1 for TBN was also located in the mQTL1–2 region, further corroborating this region. The lem1, MYB78 and opaque2 genes were located in the mQTL1–3 interval (8.5 Mb, phi308707-umc161a) for EN under two normal and two drought environments, moreover, the sQTL9 for EN was also located in this mQTL1–3 interval. The vp8 locus was detected within the mQTL1–4 interval (2.1 Mb) between umc1605 and umc1797, affecting TBN under five normal environments. Through joint-linkage mapping and genome-wide association study (GWAS), the lem1 gene (lethal embryo 1) has been shown to encode a plastid ribosomal protein S9, the mutants of which can lead to early embryo lethality in maize (Ma and Dooner 2004), but also regulate maize male inflorescence size (Wu et al. 2016). The MYB78 transcription factor also plays an important role in maize drought tolerance (Huang et al. 2013). The opaque2 gene regulates endosperm development in maize (Yuan et al. 2014). The EXG1 transgenic plants showed sterility and morphological abnormalities in rice (Furukawa et al. 2014). The ZMM4 gene is a MADS-box family gene that is involved in floral induction and inflorescence development in maize (Danilevskaya et al. 2008; Wu et al. 2016). The vp8 locus (viviparous 8) also regulates tassel development in maize (Wu et al. 2016).

On chromosome 2, the homologous MROS1 and IPO1 genes were identified within the mQTL2–1 region (4.8 Mb) between umc2403 and umc1934, affecting TBN under four normal environments. Moreover, the sQTL2 for TBN was also located in the mQTL2–1 region. The DBEs enzyme, WRI1 and MYB78 genes and homologous LOXs gene were mapped within the mQTL2–2 interval (77.8 Mb, umc131-umc1028) associated with TBN and EN under five normal and four drought environments. The homologous Hd1 locus was associated with the mQTL2–3 interval (0.8 Mb) between umc2184 and umc2214, affecting TBN under two normal environments. The MROS1 gene (male reproductive organ specific gene) is a homolog flowering time gene CONSTANS in Arabidopsis, which is expressed in the late phases of pollen development in Silene latifolia (Janousek et al. 2002). The IPO1 gene is a key regulator for branching, and also affects panicle structure in rice (Peng et al. 2014a). The specific isoamylase DBEs (pullulanase-type starch-debranching enzymes) plays a crucial role in development of endosperm in maize (Beatty et al. 1999). The WRI1

transcription factor is involved in the regulation of glycolysis and fatty acid biosynthesis in maize seed (Ding et al. 2015). Interestingly, silencing the expression of LOXs gene improves Grain qualities in rice (Roychowdhury et al. 2016). The Hd1, a major photoperiod sensitivity quantitative trait locus in rice, also appears to be a CONSTANS ortholog in Arabidopsis (Yano et al. 2000).

On chromosome 3, the opaque2 gene was found in the mQTL3–1 region (0.7 Mb) between umc2071 and umc2376, affecting EN under five normal environments. Moreover, the sQTL10 for EN was also located in the mQTL3–1 region. The OCL1 gene was associated with the mQTL3–2 interval (5.9 Mb) between umc1392 and umc1025, affecting TBN under six normal and seven drought environments. The fdl1 gene was detected within the mQTL3–3 interval (1.7 Mb) between bnlg1257 and umc2152 for EN under one normal environments. The OCL1 (outer cell layer 1) transcription factor can strongly delay in flowering time, which is correlated with ZMM4 and DLF1 (Delayed flowering 1) gens in maize (Depège-Fargeix et al. 2011). The fdl1 (fused leaves 1) gene controls organ separation in the embryo and seedling shoot, and promotes coleoptile opening in maize (La-Rocca et al. 2015).

On chromosome 4, the homologous RAT1, RAT2, and FLO-LFY genes and homologous FRRP1 protein were predicted within the mQTL4–1 interval (7.8 Mb) between umc2176 and umc1117, affecting TBN under three normal and three drought environments. The ZAG3 gene and homologous LOX gene were found within the mQTL4–2 region (9.2 Mb) between bnlg1621a-bnlg1784, affecting TBN and EN under six normal environments. The sQTL11 for EN further corroborated this region involvement. The homologous SPL3 and LOXs genes, and the CaMBP gene were found in the mQTL4–3 region (4.3 Mb) between umc2287 and umc1101, affecting TBN under two normal and one drought environments, and was further corroborated by sQTL3. The RAT1 and RAT2 are genes related to acetyltransferase in Arabidopsis, and the RAT2-knock-out/RAT1-knock-down (RNAi) lines (r2/r1i) displayed retarded growth and delayed development, even the r2/r1i lines flowered late under long day conditions (Wang 2009). The FLO-LFY gene down-regulates panicle branch initiation in rice (Kyozuka et al. 1998). The FRRP1 (flowering-regulated ring protein 1) regulates flowering time and yield potential in rice by affecting histone H2B mono-

ubiquitination (Du et al. 2016). The ZAG3 gene clusters with MADS-box genes to regulate the floral meristem and determine the fate of floral organ primordia in maize (Mena et al. 1995; Wu et al. 2016). The SPL3 gene is in the BSP-box gene family, which regulates inflorescence apical meristems, floral meristems, and floral organ primordia in Arabidopsis (Cardon et al. 1997). The CaMBP protein plays important role in regulating abiotic stress (drought stress, salt stress and low temperature stress, etc.) in multiple plants (Mao et al. 2004).

On chromosome 5, the homologous SNAC3 transcription factor was detected within the mQTL5–1 region (2.9 Mb) between umc2216 and umc1072, affecting TBN under one normal and one drought environments. Furthermore, this gene regulates drought and heat tolerance through the modulation of reactive oxygen species in rice (Fang et al. 2015). Moreover, the sQTL4 for TBN was also located in the mQTL5–1 region.

On chromosome 6, the Ig3, EF-1 alpha and GST genes were mapped within the mQTL6–1 interval (11.1 Mb) between umc2040 and bnlg1174a, affecting EN under two normal and four drought environments. The sQTL12 for EN was also located in this interval. The Ig3 gene regulates tassel development in maize (Wu et al. 2016), while the EF-1 alpha and GST genes are involved in multiple abiotic stress, especially during drought stress in maize (McGonigle et al. 2000).

On chromosome 7, the homologous MADS3 and OsCIN1 genes, and HSP3 protein were detected within the mQTL7–1 region (1.6 Mb) between umc2177 and umc1378, affecting TBN under two normal and four drought environments. The sQTL6 for TBN was also located in this region. The Ig3 gene and E1 enzyme were identified within the mQTL7–2 interval (8.7 Mb) between umc1710 and umc1295a for TBN under two normal and one drought environments. The mQTL7–2 interval was also associated with the sQTL7. The MADS3 gene regulates late anther development and pollen formation in rice (Hu et al. 2011; Wu et al. 2016). The OsCIN1 (cell-wall invertase gene 1) rapidly halts anthesis and peduncle elongation in rice under water deficit (Ji et al. 2005). The HSP3 (heat shocked protein) improves drought resistance in maize (Song et al. 2014). The E1 (ubiquitin-activating enzyme 1) is involved in stress resistance maize (Wang et al. 2010).

On chromosome 8, the homologous ald1and OsSIK2 genes, and ig1 gene were mapped within the mQTL8–1

region (2.3 Mb) between bnlg240 and mmc0181, affecting EN under two drought environments. The *ald1* (aldolase 1) gene regulates development of endosperm in rice (Lai et al. 2004). The *ig1* (indeterminate gametophyte 1) gene restricts the proliferative phase of female gametophyte development in maize, and *ig1* mutant female gametophytes have a prolonged phase of free nuclear divisions leading to a variety of embryo sac abnormalities (Evans 2007). The *OsSIK2* (S-domain receptor-like kinase 2) is involved in multiple abiotic stress responses and the senescence process in rice (Chen et al. 2013).

On chromosome 9, the *ZAG4* gene was identified within the mQTL9–1 interval (1.6 Mb) between umc1588 and umc1170, affecting TBN under three normal environments. The *ZAG4* is a *MADS*-box gene that regulates the floral meristem and determines the fate of floral organ primordia in maize (Mena et al. 1995; Wu et al. 2016).

On chromosome 10, the *cr4* (crinkly 4) gene was mapped within the mQTL10–1 region (2.2 Mb) between bnlg1451 and phi063, affecting EN under one normal environment. The *cr4* is a TNFR-like receptor kinase and involved in development of endosperm surface in maize (Becraft et al. 1996).

Conclusion

Here, we developed two $F_{2:3}$ populations (LTpop and CTpop) to identify 19 QTLs for TBN and EN under eight different watering environments by single environment mapping with CIM, and 11/19 QTLs were identified under water-stressed environments. Then 21 QTLs were identified in the two $F_{2:3}$ populations via joint analysis across all environments with MCIM, 11/21 QTLs were involved in QTL × E interactions. Demonstrating that inflorescence architecture traits (TBN and EN) in maize are complex traits controlled by many genes of major or minor effects, and these identified QTLs will facilitate the elucidation of inflorescence architecture molecular mechanism under different watering environments.

Moreover, seven pairs of epistatic interactions for TBN and EN were identified with AA or AD effects in the two $F_{2:3}$ populations among all environments. Suggesting that the epistasis will play fundamental roles in broadening our understanding of the genetic structure behind inflorescence architecture in maize. Twelve

sQTLs were also identified in the two $F_{2:3}$ populations by single environment mapping with CIM and joint analysis through MCIM. Showing that these sQTLs confirm the importance and relevance of inflorescence architecture in maize breeding for drought tolerance.

In addition, 20 mQTLs for TBN and EN were identified across 19 populations under 51 watering environments via a meta-analysis, and 34 candidate genes were identified in corresponding mQTLs regions. Suggesting that the systems-level integration and re-analysis of fruitful QTL data provide useful information for QTL cloning and breeding applications.

Compliance with ethical standards

Conflict of interest The authors declare that they have no conflict of interest.

References

Agrama HAS, Moussa ME (1996) Mapping QTLs in breeding for drought tolerance in maize (*Zea mays* L.) Euphytica 91:89–97

Almeida GD, Nair S, Borém A, Cairns J, Trachsel S, Ribaut JM, Bänziger M, Prasanna BM, Crossa J, Babu R (2014) Molecular mapping across three populations reveals a QTL hotspot region on chromosome 3 for secondary traits associated with drought tolerance in tropical maize. Mol Breed 34: 701–715

Bartlett ME, Thompson B (2014) Meristem identify and phyllotaxis in inflorescence development. Front Plant Sci 14(5):508

Beatty MK, Rahman A, Cao H, Woodman W, Lee M, Myers AM, James MG (1999) Purification and molecular genetic characterization of ZPU1, a pullulanase-type starch-debranching enzyme from maize. Plant Physiol 119(1):255–266

Becraft PW, Stinard PS, McCarty DR (1996) CRINKLY4: a TNFR-like receptor kinase involved in maize epidermal differentiation. Science 273(5280):1406–1409

Brown PJ, Upadyayula N, Mahone GS, Tian F, Bradbury PJ, Myles S, Holland JB, Flint-Garcia S, Mcmullen MD, Buckler ES, Rocheford TR (2011) Distinct genetic architectures for male and female inforescence traits of maize. PLoS Genet 7(11):e1002383

Cardon GH, Hohmann S, Nettesheim K, Saedler H, Huijser P (1997) Functional analysis of the *Arabidopsis thaliana* SBP-box gene SPL3: a novel gene involved in the floral transition. Plant J 12(2):367–377

Chen LJ, Wuriyanghan H, Zhang YQ, Duan KX, Chen HW, Li QT, Lu X, He SJ, Ma B, Zhang WK, Lin Q, Chen SY, Zhang JS (2013) An S-domain receptor-like kinase, OsSIK2,

confers abiotic stress tolerance and delays dark-induced leaf senescence in rice. Plant Physiol 163(4):1752–1765

Chen ZL, Wang BB, Dong XM, Liu H, Ren LG, Chen J, Hauck A, Song WB, Lai JS (2014) An ultra-high density bin-map for rapid QTL mapping for tassel and ear architecture in a large F$_2$ maize population. BMC Genomics 15:433

Churchill GA, Doerge RW (1994) Empirical threshold values for quantitative trait mapping. Genetics 138:963–971

Danilevskaya ON, Meng X, Selinger DA, Deschamps S, Hermon P, Vansant G, Gupta P, Ananiev EV, Muszynski MG (2008) Involvement of the MADS-box gene ZMM4 in floral induction and inflorescence development in maize. Plant Physiol 147(4):2054–2069

Darvasi A, Soller M (1997) A simple method to calculate resolving power and confidence interval of QTL map location. Behav Genet 27:125–132

Depège-Fargeix N, Javelle M, Chambrier P, Frangne N, Gerentes D, Perez P, Rogowsky PM, Vernoud V (2011) Functional characterization of the HD-ZIP IV transcription factor OCL1 from maize. J Exp Bot 62(1):293–305

Ding X, Yang SQ, Xu Q, Du CF, Wu SJ, Luo XL, Ma YB, Zhang AH, Sun X, Li PB (2015) Progress on transcription factor WRI1 in crops. Mol Plant Breed 13(3):697–701

Dong YB, Zhang ZW, Shi QL, Wang QL, Zhou Q, Deng F, Ma ZY, Qiao DH, Li YL (2015) QTL consistency for agronomic traits across three generations and potential applications in popcorn. J Integr Agric 14(12):2547–2557

Du Y, He W, Deng C, Chen X, Gou L, Zhu F, Guo W, Zhang J, Wang T (2016) Flowering-related RING protein 1 (FRRP1) regulates flowering time and yield potential by affecting histone H2B monoubiquitination in rice (Oryza sativa). PLoS One 11(3):e0150458

Duvick DN, Cassman KG (1999) Post-green revolution trends in yield potential of temperate maize in the north-Central United States. Crop Sci 39:1622–1630

Duvick DN, Smith JSC, Cooper M (2004) Long-term selection in commercial hybrid maize breeding program. Plant Breed Rev 24:109–151

EI-Soda M, Boer MP, Bagheri H, Hanhart CJ, Koornneef M, Aarts MG (2014) Genotype-environment interactions affecting preflowering physiological and morphological traits of Brassica rapa grown in two watering regimes. J Exp Bot 65(2):697–708

Evans MM (2007) The indeterminate gametophyte 1 gene of maize encodes a LOB domain protein required for embryo sac and leaf development. Plant Cell 19(1):46–62

Fan JJ, Wang NZ, Zhu YS, Cui ZH, Yuan YH, Zhang LJ (2012) Research progress on prolificacy in maize. J Maize Sci 20(5):143–146

Fang Y, Liao K, Du H, Xu Y, Song H, Li X, Xiong L (2015) A stress-responsive NAC transcription factor SNAC3 confers heat and drought tolerance through modulation of reactive oxygen species in rice. J Exp Bot 66(21):6803–6817

Furukawa K, Ichikawa S, Nigorikawa M, Sonoki T, Ito Y (2014) Enhanced production of reducing sugars from transgenic rice expressing exoglucanase under the control of a senescence-inducible promoter. Transgenic Res 23(3):531–537

Gao SB, Zhao MJ, Lan H, Zhang ZM (2007) Identification of QTL associated with tassel branch number and total tassel length in maize. Yi Chuan 29(8):1013–1017

Gowda M, Kling C, Würschum T, Reif JC (2010) Hybrid breeding in durum wheat: heterosis and combining ability. Crop Sci 50:2224–2230

Heyl A, Muth J, Santandrea G, O'Connell T, Serna A, Thompson RD (2001) A transcript encoding a nucleic acid-binding protein specifically expressed in maize seeds. Mol Gen Genomics 266(2):180–189

Hu YM, Wu X, Li CX, Fu ZY, Liu ZH, Tang JH (2008) Genetic analysis on the related traits of florescence for hybrid seed production in maize. J Nanjing Agric Univ 31(1):11–16

Hu LF, Liang WQ, Yin CS, Cui X, Zong J, Wang X, Hu JP, Zhang DB (2011) Rice MADS3 regulates ros homeostasis during late anther development. Plant Cell 23:515–533

Hu HL, Liu QH, Xia YL, Li TF, Zhang K (2012) Discussions on ear malformation of maize and its control method. J Jilin Agric Sci 37(1):21–22

Huang C, Hu G, Li Y, Wu J, Zhou X (2013) NbPHAN, a MYB transcriptional factor, regulates leaf development and affects drought tolerance in Nicotiana Benthamiana. Physiol Plant 149(3):297–309

Huo D, Ning Q, Shen X, Liu L, Zhang Z (2016) QTL mapping of kernel number-related traits and validation of one major QTL for ear length in maize. PLoS One 11(5):e0155506

Janousek B, Matsunaga S, Kejnovsky E, Ziuvova J, Vyskot B (2002) DNA methylation analysis of a male reproductive organ specific gene (MPOS1) during pollen development. Genome 45(5):930–938

Ji XM, Raveendran M, Oane R, Ismail A, Lafitte R, Bruskiewich R, Cheng SH, Bennett J (2005) Tissue-specific expression and drought responsiveness of cell-wall invertase genes of rice at flowering. Plant Mol Biol 59(6):945–964

Knapp SJ, Stroup WW, Ross WM (1985) Exact confidence intervals for heritability on a progeny mean basis. Crop Sci 25:192–194

Kyozuka J, Konishi S, Nemoto K, Izawa T, Shimamoto K (1998) Down-regulation of RFL, the FLO/LFY homolog of rice, accompanied with panicle branch initiation. Proc Natl Acad Sci USA 95(5):979–1982

Lai J, Dey N, Kim CS, Bharti AK, Rudd S, Mayer KF, Larkins BA, Becraft P, Messing J (2004) Characterization of the maize endosperm transcriptome and its comparison to the rice genome. Genome Res 14(10A):1932–1937

Lambert RJ, Ohnson RR (1978) Leaf angle, tassel morphology, and the performance of maize hybrids. Crop Sci 18:499–502

Lan JH (2010) QTL analysis on the flowering related traits in maize. Acta Botan Boreali-Occiden Sin 30(3):0471–0480

La-Rocca N, Manzotti PS, Cavaiuolo M, Barbante A, Dalla-Vecchia F, Gabotti D, Gendrot G, Horner DS, Krstajic J, Persico M, Rascio N, Rogowsky P, Scarafoni A, Consonni G (2015) The maize fused leaves 1 (fdl1) gene controls organ separation in the embryo and seedling shoot and promotes coleoptile opening. J Exp Bot 66(19):5753–5767

Li XH, Li XH, Hao ZF, Tian QZ, Zhang SH (2005) Consensus map of the QTL relevant to drought tolerance of maize under drought conditions. Sci Agric Sin 38(5):882–890

Li NN, Yang JZ, Hao JP (2011) Influence of nutrients and density stress on ear high dimensional size of growing ear and its relation to kernel yield in corn. J Nuclear Agri Sci 25(3):0563–0569

Lu M, Zhou F, Xie CX, Li MS, Li XH, Yang XJ, Liu MZ, Zhang SH (2007) Analysis of epistatic and QTL x E interaction of ear length in maize. Crops 4:30–32

Ma Z, Dooner HK (2004) A mutation in the nuclear-encoded plastid ribosomal protein S9 leads to early embryo lethality in maize. Plant J 37(1):92–103

Ma XQ, Tang JH, Teng WT, Yan JB, Meng YJ, Li JS (2007) Epistatic interaction is an important genetic basis of grain yield and its components in maize. Mol Breed 20(1):41–51

Mao GH, Song LX, Sun DY (2004) Progress of study on calmodulin-binding proteins in plants. J Plant Physiol Mol Biol 30(5):481–488

McCouch SR, Cho GY, Yano M, Paul E, Blinstrub M, Morishima H, Kinoshita T (1997) Report on QTL nomenclature. Rice Genet Newsletter 14:11–13

McGonigle B, Keeler SJ, Lau SM, Koeppe MK, O'Keefe DP (2000) A genomics approach to the comprehensive analysis of the glutathione s-transferase gene family in soybean and maize. Plant Physiol 124(3):1105–1120

Mena M, Mandel MA, Lerner DR, Yanofsky MF, Schmidt RJ (1995) A characterization of the MADS-box gene family in maize. Plant J 8(6):845–854

Michael L (1999) Estimating genetic correlations in natural populations. Genet Res Camb 74:255–264

Mickelson SM, Stuber CS, Senior L, Kaeppler SM (2002) Quantitative trait loci controlling leaf and tassel traits in a B73 x Mo17 population of maize. Crop Sci 42:1902–1909

Nikolic A, Andjelkovic V, Dodig D, Ignjatovia-Micic D (2011) Quantitative trait loci for yield and morphological traits in maize under drought stress. Genetika 43(2):263–276

Peng YL, Zhao XQ, Ren XW, Li JY (2013) Effect of drought stress on growth of different plant type maize (Zea mays) in the bell-mouthed period. J Desert Res 33(4):1064–1070

Peng Y, Gao Z, Zhang B, Liu C, Xu J, Ruan B, Hu J, Dong G, Guo L, Liang G, Qian Q (2014a) Fine mapping and candidate gene analysis of a major QTL for panicle structure in rice. Plant Cell Rep 33(11):1843–1850

Peng YL, Zhao XQ, Ren XW, Li JY (2014b) Genotypic difference in response of physiological characteristics and grain yield of maize inbred lines to drought stress at flowering stage. Agric Res Arid Areas 32(3):9–14

Phillips PC (2008) Epistasis-the essential role of gene interactions in the structure and evolution of gene interactions in the structure and evolution of genetic systems. Nat Rev Genet 9(11):855–867

Ribaut JM, Jiang C, Gonzalez-de-leon D, Edmeades GO, Hoisington DA (1997) Identification of quantitative trait loci under drought conditions in tropical maize. 2. Yield components and marker-assisted selection strategies. Theor Appl Genet 94:887–896

Ritchie SW, Hanway JJ, Benson GO (1997) How a corn plant develops. Spec. Rep. 48. Iowa State Univ. Coop. Ext. Serv., Ames, IA

Ross AJ, Hallauer AR, Lee M (2006) Genetic analysis of traits correlated with maize ear length. Maydica 51:301–313

Roychowdhury M, Li X, Qi H, Li W, Sun J, Huang C, Wu D (2016) Functional characterization of 9–13-LOXs in rice and silencing their expression to improve grain qualities. Biomed Res Int 4275904

Saghai-Maroof MA, Soliman KM, Jorgensen RA, Allard RW (1984) Ribosomal DNA spacer-length polymorphisms I barley:

Mendelian inheritance, chromosomal locations, and population dynamics. Proc Natl Acad Sci U S A 81:8014–8018

Schoper JB, Lambert RJ, Vasilas BL, Westgate ME (1987) Plant factors controlling seed set in maize: the influence of silk, pollen, and ear-leaf water status and tassel heat treatment at pollination. Plant Physiol 83(1):121–125

Song FB, Dai JY (2005) Response and adaptability of maize to drought stressII. Response of ear and tassel growth and development of maize to drought stress. J Jilin AgriUniv 27(1):1–5

Song A, Zhu X, Chen F, Gao H, Jiang J, Chen S (2014) A chrysanthemum heat shock protein confers tolerance to abiotic stress. Int J Mol Sci 15(3):5063–5078

Sosnowski O, Joets J (2012) BioMercator v4 user guide. UMR de Génétique Végétale du MoulonF- 91190 Gif-sur-Yvette (http://www.bioinformatics.org/mqtl/wiki)

Stuber CW, Edwards MD, Wendel J (1987) F1 molecular marker facilitated investigations of quantitative trait loci in maize. II. Factors influencing yield and its component traits. Crop Sci 27:639–648

Sun Z, Mo QC, Cheng BJ, Xie CX, Lin F (2012) Analysis of inheritance, heterosis and parent-off spring correlation of tassel branch number in maize (Zea mays L.) Crops 2:31–35

Tanaka W, Pautler M, Jackson D, Hirano HY (2013) Grass meristems II: inflorescence architecture, flower development and meristem fate. Plant Cell Physiol 54:313–324

Tang H, Yan JB, Huang YQ, Zheng YL, Li JS (2005) QTL mapping of five agronomic traits in maize. Acta Genet Sin 32(2):203–209

Trachsel S, Messmer R, Stamp P, Hund A (2009) Mapping of QTLs for leteral and axile root growth of tropical maize. Theor Appl Genet 119:1413–1424

Upadyayula N, da Silva HS, Bohn MO, Rocheford TR (2006) Genetic and QTL analysis of maize tassel and ear inflorescence architecture. Theor Appl Genet 112:592–606

Van-Ooijen JW (2006) JoinMap® 4: software for the calculation of genetic linkage maps in experimental populations. Kyazma BV (http://www.kyazma.nl/index.php/mc.JoinMap/sc.Evaluate/)

Veldboom LR, Lee M (1994) Molecular-marker-facilitated studies of morphological traits in maize. II: determination of QTLs for grain yield and yield components. Theor Appl Genet 89:451–458

Wang Q (2009) A molecular genetics study of the related to acetyltransferase 1 and 2 (RAT1 and RAT2) genes. Hunan University

Wang S, Basten CJ, Zeng ZB (2007) Windows QTL Cartographer 2.5. Department of Statistics, North Carolina State University, Raleigh, NC. (http://statgen.ncsu.edu/qtlcart/WQTLCart.htm)

Wang JL, Shi Shi SQ, Jia LQ, Jiang ZP (2010) Progress on functions of ubiquitin conjugating enzyme (E2) in plants. Biotechnol Bull 4:7–10

Wang D, Li YX, Wang Y, Liu C, Liu ZZ, Peng B, Tan WW, Zhang Y, Sun BC, Shi YS, Song YC, Wang TY, Li Y (2011) Major quantitative trait loci analysis of tassel primary branch number and tassel weight in maize (Zea mays). Chin Bull Bot 46(1):11–20

Wu X, Li Y, Shi Y, Song Y, Zhang D, Li C, Buckler ES, Li Y, Zhang Z, Wang T (2016) Joint-linkage mapping and GWAS reveal extensive genetic loci that regulate male inflorescence size in maize. Plant Biotechnol J 14(7):1551–1562

Xu J, Yuan Y, Xu Y, Zhang G, Guo X, Wu F, Wang Q, Rong T, Pan G, Cao M, Tang Q, Gao S, Liu Y, Wang J, Lan H, Lu Y (2014) Identification of candidate genes for drought tolerance by whole-genome resequencing in maize. BMC Plant Biol 14:83

Yang C, Tang DG, Zhang L, Liu J, Rong TZ (2015) Identification of QTL for ear row number and two ranked versus many-ranked ear in maize across four environments. Euphytica 206:33–47

Yang C, Zhang L, Jia A, Rong T (2016) Identification of QTL for maize grain yield and kernel-related traits. J Genet 95(2): 239–247

Yano M, Katayose Y, Ashikari M, Yamanouchi U, Monna L, Fuse T, Baba T, Yamamoto K, Umehara Y, Nagamura Y, Sasaki T (2000) Hd1, a major photoperiod sensitivity quantitative trait locus in rice, is closely related to the Arabidopsis flowering time gene CONSTANS. Plant Cell 12(12):2473–2484

Yuan L, Dou Y, Kianian SF, Zhang C, Holding DR (2014) Deletion mutagenesis identifies a haploinsufficient role for γ-zein in opaque2 endosperm modification. Plant Physiol 164(1):119–130

Zhang YJ, Jiang F, Liu PF, Zhang ZL, Chen QC, Wang XM (2013) QTL mapping for tassel primary branch number in sweet corn. Hubei Agri Sci 52(15):3492–3495

Zhang ZL, Jiang F, Liu PF, Chen QC, Zhang Y, Wang XM (2014) QTL mapping for tassel primary branch number in sweet corn. J South China Agri Univ 35(1):110–113